Article

Cell

G1/S Inhibitors and the SWI/SNF Complex Control Cell-Cycle Exit during Muscle Differentiation

Graphical Abstract

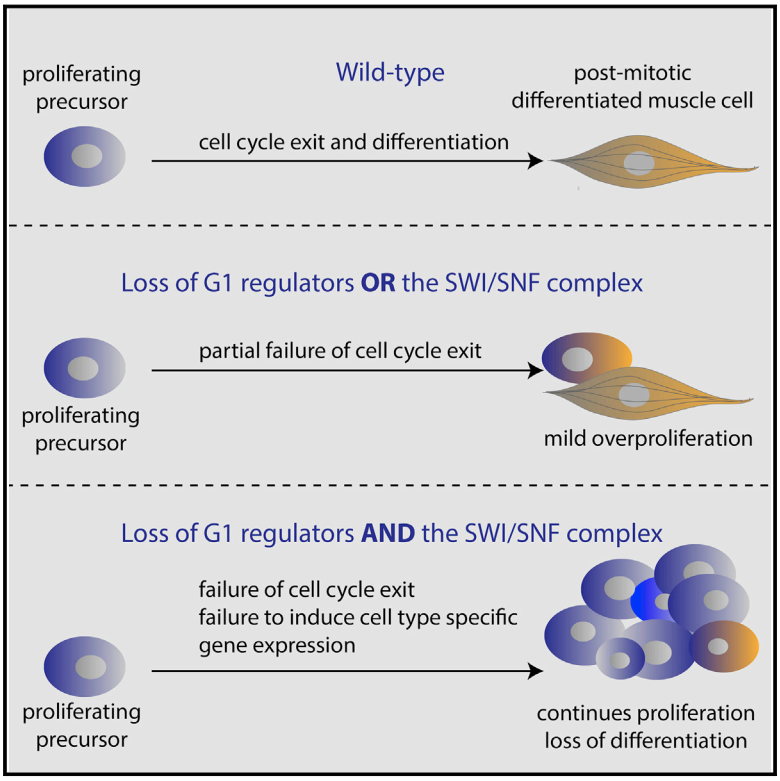

Authors

Suzan Ruijtenberg, Sander van den Heuvel

Correspondence

s.j.l.vandenheuvel@uu.nl

In Brief

SWI/SNF-mediated chromatin remodeling provides an important brake on cell proliferation in *C. elegans*, suggesting an explanation for frequent mutation of this complex in human tumors.

Highlights

- A combined conditional knockout and lineage-tracing system for *C. elegans*
- Quantitative in vivo analysis of cell-cycle exit during development
- SWI/SNF and G1/S inhibitors provide alternative mechanisms for cell-cycle arrest
- The SWI/SNF complex prevents tumorous over-proliferation in *C. elegans*

Ruijtenberg & van den Heuvel, 2015, Cell *162*, 300–313
July 16, 2015
http://dx.doi.org/10.1016/j.cell.2015.06.013

CellPress

Cell

Article

G1/S Inhibitors and the SWI/SNF Complex Control Cell-Cycle Exit during Muscle Differentiation

Suzan Ruijtenberg[1] and Sander van den Heuvel[1,*]
[1]Developmental Biology, Department of Biology, Faculty of Sciences, Utrecht University, Padualaan 8, 3584 CH Utrecht, the Netherlands
*Correspondence: s.j.l.vandenheuvel@uu.nl
http://dx.doi.org/10.1016/j.cell.2015.06.013

SUMMARY

The transition from proliferating precursor cells to post-mitotic differentiated cells is crucial for development, tissue homeostasis, and tumor suppression. To study cell-cycle exit during differentiation in vivo, we developed a conditional knockout and lineage-tracing system for *Caenorhabditis elegans*. Combined lineage-specific gene inactivation and genetic screening revealed extensive redundancies between previously identified cell-cycle inhibitors and the SWI/SNF chromatin-remodeling complex. Muscle precursor cells missing either SWI/SNF or G1/S inhibitor function could still arrest cell division, while simultaneous inactivation of these regulators caused continued proliferation and a *C. elegans* tumor phenotype. Further genetic analyses support that SWI/SNF acts in concert with *hlh-1* MyoD, antagonizes Polycomb-mediated transcriptional repression, and suppresses *cye-1* Cyclin E transcription to arrest cell division of muscle precursors. Thus, SWI/SNF and G1/S inhibitors provide alternative mechanisms to arrest cell-cycle progression during terminal differentiation, which offers insight into the frequent mutation of SWI/SNF genes in human cancers.

INTRODUCTION

The development and maintenance of tissues and organisms depend on close coordination between cell proliferation and differentiation. Early embryos contain rapidly proliferating totipotent cells, whereas adult tissues predominantly consist of non-dividing cells with specialized morphologies and functions (Buttitta and Edgar, 2007). In general, cell specialization involves a gradual process of lineage restriction, followed by permanent exit from the division cycle and terminal differentiation. The mechanisms that arrest cell proliferation during differentiation are crucial for tumor suppression but limit tissue regeneration. Despite this importance, it remains poorly understood how cell proliferation and differentiation are inversely regulated during development, and how temporary quiescence differs from permanent cell-cycle arrest.

The primary mechanism to arrest cell division is inhibition of cyclin-dependent kinases (CDKs), the key positive regulators of the cell division cycle. CDK4/6-cyclin D and CDK2-cyclin E kinases promote cell-cycle entry during the G1 phase of the cell cycle (van den Heuvel and Dyson, 2008). Various levels of regulation counteract CDK-cyclin activation to prevent unscheduled progression from G1 into S phase. G1/S inhibitors include members of the retinoblastoma tumor suppressor (Rb) protein family, which act as transcriptional repressors together with E2F transcription factors. Phosphorylation of pRb by active CDKs triggers its release from E2F and allows activating E2Fs to induce transcription of cyclin E and other cell-cycle genes. In addition, CDK inhibitory proteins (CKIs) oppose G1/S progression. CKIs of the INK4 protein family, such as $p16^{INK4A}$, associate with CDK4/6 kinases and prevent their interaction with D-type cyclins. In contrast, CKIs of the CIP/KIP family associate with CDK-cyclin complexes and are particularly important for inhibiting CDK2-cyclin E. Ubiquitin-dependent protein degradation provides yet another level of G1/S inhibition. This involves the Anaphase Promoting Complex/Cyclosome (APC/C) in association with the FZR1/Cdh1 coactivator, as well as Skp1, Cullin, F-box factor (SCF) complexes. APC/C and SCF are both E3 ubiquitin ligases that target cell-cycle regulatory proteins for degradation.

Cell differentiation is ultimately determined at the level of gene expression. As a well-studied example, muscle differentiation involves a regulatory network of MyoD and other myogenic transcription factors, together with general transcription factors and histone modification/chromatin remodeling complexes (Puri and Mercola, 2012). Other transcription factors mediate differentiation into, for instance, specific blood cell types or neurons. Mutations associated with human cancer frequently affect cell-cycle regulators, but also transcription factors and chromatin regulators with critical functions in differentiation (Kandoth et al., 2013). In particular, transcriptional repressors and activators of the polycomb group (PcG) and Trithorax group (TrxG), respectively, are strongly associated with cell fate and tumor formation. In fact, mutations in a subclass of TrxG genes, which encode subunits of Switch/Sucrose nonfermentable (SWI/SNF) chromatin remodeling complexes, were recently found among the most common mutations in human cancer (Kadoch et al., 2013; Kandoth et al., 2013; Wang et al., 2014). These findings highlight the importance of understanding how the combinatorial activity of cell-cycle regulators, transcription factors, and chromatin remodelers coordinate cell-cycle arrest and differentiation.

The nematode *Caenorhabditis elegans* provides an attractive animal system in which to study the control of cell-cycle exit during development. *C. elegans* develops through a highly reproducible pattern of cell proliferation and differentiation (Sulston

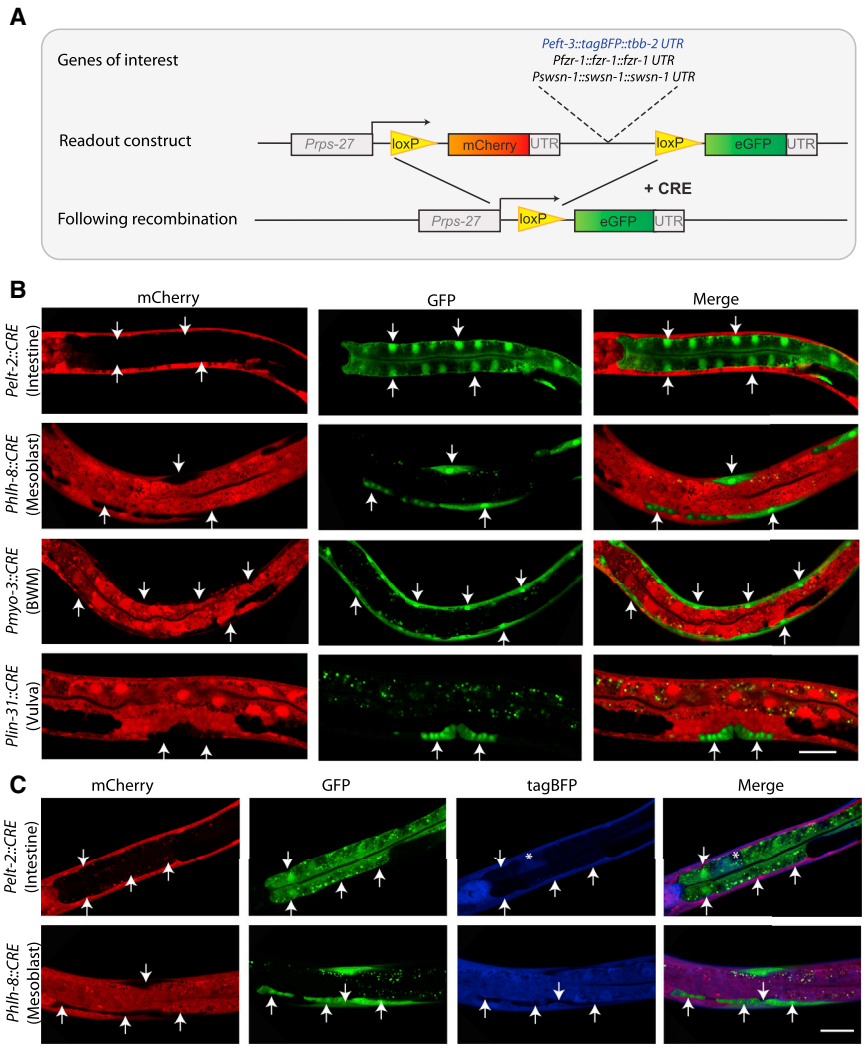

Figure 1. Lineage Tracing and Tissue-Specific Knockout in *C. elegans*

(A) Overview of the CRE-lox based recombination system, which combines tissue-specific gene inactivation with switching mCherry to eGFP expression to allow lineage tracing. The single-copy integrated plasmid without gene of interest is used as a recombination reporter (*readout*^{lox}). *Peft-3::tagBFP*, *swsn-1*, and *fzr-1* were studied as genes of interest.

(B) Examples of lineage-specific recombination and lineage tracing following tissue-specific CRE expression from the indicated promoters. Arrows indicate cells that switched mCherry to eGFP expression.

(C) CRE-lox-based recombination causes loss of expression of a *tagBFP* reporter gene of interest (A), single copy integrated into the genome. CRE expressed from the indicated promoters resulted in loss of mCherry and tagBFP expression, while eGFP was induced (indicated by arrows). Asterisk (*) indicates mCherry-negative intestinal cell with residual tagBFP fluorescence.

Scale bar, 20 μm. See also Figures S1 and S2 and Tables S1 and S2.

and Horvitz, 1977; Sulston et al., 1983). The animal's transparency and well-described lineage allow characterization of mutants with single-cell resolution. Extra cell division (hyperplasia) of somatic cells was first observed in the lineage-abnormal mutants *lin-23* β-TrCP and *cul-1* (*lin-19*), which lack the function of an SCF-like E3 ubiquitin ligase (Kipreos et al., 1996, 2000). Loss of *cki-1* Kip1 also results in extra cell division (Boxem and van den Heuvel, 2001; Fukuyama et al., 2003; Hong et al., 1998). In contrast, mutation of the single *C. elegans* Rb-related gene, *lin-35*, or the APC/C coactivator *fzr-1* FZR1/Cdh1 leads to substantial hyperplasia only when combined with loss of other negative cell-cycle regulators (Boxem and van den Heuvel, 2001; Fay et al., 2002). Notably, such double mutants still form apparently normal differentiated post-mitotic cells, and uncontrolled over-proliferation of somatic cells has thus far not been described for *C. elegans*.

To study cell-cycle arrest during the process of differentiation, we created a system for tissue-specific gene inactivation and lineage tracing. This allowed inactivation of multiple genes in a single precursor cell, while fluorescently marking all daughter cells. Combining this system with RNAi of candidate genes revealed multiple levels of control that together provide robust arrest of cell division during terminal differentiation. We observed a surprising degree of redundancy between well-known negative regulators of the cell cycle and the SWI/SNF chromatin-remodeling complex. Only combined inactivation of the SWI/SNF complex and G1/S inhibitors resulted in tumorous over-proliferation of muscle precursor cells. Our results support that SWI/SNF-dependent chromatin remodeling provides global transcriptional control not only of cell-type-specific genes, but also of positive and negative cell-cycle regulators. This provides an alternative mechanism for control of cell-cycle exit during terminal differentiation and likely is relevant for the tumor suppressor function of SWI/SNF genes.

RESULTS

A CRE-Lox Based Recombination and Lineage-Tracing System for *C. elegans*

We assumed that cell-cycle withdrawal during differentiation depends on multiple regulators and is essential for viability. Hence, to genetically dissect developmental control of cell-cycle exit, we aimed to induce multiple gene alterations in a lineage-specific manner. Hereto, we developed a CRE-lox-based recombination and lineage-tracing system for *C. elegans* (Figure 1A). This system combines a recombination vector that includes a gene of interest, a homozygous genomic mutation of the gene, and tissue-specific expression of the CRE recombinase. This allows tissue-specific gene loss and simultaneous

visualization of knockout cells by altered expression of fluorescent proteins.

We started with a recombination-reporter (*readout^{lox}*) construct that expresses the mCherry fluorescent protein from the universally active ribosomal subunit *rps-27* promoter (Figure 1A). *LoxP* recombination sites were placed upstream of the mCherry coding sequences and downstream of a polyadenylation/transcriptional stop signal (*let-858* 3′ UTR). This is followed by eGFP coding sequences without promoter, causing CRE-induced recombination to induce a switch from mCherry to eGFP expression (Figure 1A, bottom). Following extensive optimization of the CRE-expressing vectors (Supplemental Experimental Procedures), recombination was highly efficient and observed in nearly all animals with a *readout^{lox}* construct (Table S1).

To examine conditional recombination, we expressed CRE under the control of a heat-shock-inducible promoter (*Phsp-16.2*) and a variety of promoters with lineage-specific activity. Recombination was readily detected by expression of eGFP, coincident with mCherry loss, and occurred in the expected lineages in nearly all animals (Figure 1B; data not shown). Dependent on the promoter used, additional cell types sometimes showed eGFP expression (Table S1). For instance, early embryonic expression of CRE from the *elt-2* GATA4-6 and *hlh-8* TWIST promoters induced recombination as expected in the intestine and mesoblast (M) lineage, respectively. However, both promoters showed some additional activity in the somatic gonad, and *Phlh-8::CRE* also induced recombination in embryonic body-wall muscles (BWM), mostly in the head region of the animal. In practice, this level of transcriptional noise did not pose a problem as it usually caused recombination of only one allele (as concluded from coincident mCherry and eGFP expression) in a few specific cells.

Several adjustments expanded the versatility of the system. We introduced alternative lox sites (*loxP*, *loxN*, and *lox2272*) for reliable recombination of multiple genes in the same cell (Figure S1; Table S2). Moreover, we created readout constructs that switch from mCherry to tagBFP expression, to allow lineage tracing in combination with use of GFP-reporter transgenes (Figure S1). Finally, we tested whether CRE-induced recombination is likely to cause loss of function of the gene of interest. DNA injected into the *C. elegans* gonad regularly forms multi-copy arrays that remain present extra-chromosomally (Mello et al., 1991). To exclude that CRE-lox excised DNA fragments are retained through a similar mechanism, we placed tagBFP coding sequences flanked by a general promoter (*Peft-3*) and 3′ UTR (*tbb-2* UTR) between the *loxP* sites in the recombination vector (Figure 1A). Genomic integration of this vector resulted in animals with mCherry and tagBFP expression in all somatic cells. Lineage-specific CRE expression resulted in loss of mCherry and tagBFP expression (Figure 1C), although tagBFP fluorescence lasted somewhat longer than mCherry fluorescence. Recombination could be induced even in post-mitotic cells, based on eGFP expression and mCherry loss in body-wall muscle, but tagBFP expression perdured in these cells (Figure 1B; Figure S2). Thus, cell division likely helps creating a loss of gene function with this approach. In the intestine and mesoblast lineages, tagBFP was completely absent in all later stage larvae examined. In summary, CRE-lox-mediated recombination allows efficient lineage-specific loss of function in *C. elegans*, and knockout cells can be readily visualized based on fluorescent protein expression.

General Inhibitors of G1/S Progression Show Lineage-Dependent Contributions

We focused our analysis of cell-cycle exit on the intestine and post-embryonic mesoderm lineage of the mesoblast. Nuclear divisions in the intestine are sensitive to cell-cycle deregulation (Boxem and van den Heuvel, 2001, 2002; Korzelius et al., 2011; Saito et al., 2004), while the M lineage is particularly attractive for proliferation-differentiation studies. The mesoblast (M) is formed at approximately 4 hr of embryonic development and remains quiescent until halfway the first larval stage (L1) (Sulston et al., 1983) (Figure 2A). Cell divisions in L1 generate 16 M daughter cells that undergo terminal differentiation, and two ventral precursor cells known as sex myoblasts (SMs). The SMs migrate anteriorly to align with the gonad during L2 development (Figures 2A and 2B) (Sulston and Horvitz, 1977). Starting in the late L3 stage, each SM goes through three rounds of division to form a total of 16 vulval and uterine muscles that are used for egg laying and are known as sex muscles. Thus, the M lineage includes multiple periods of proliferation, temporal arrest, and terminal differentiation over a substantial part of the animal's development.

We first examined whether the *lin-35* Rb and *fzr-1* FZR1/Cdh1 inhibitors of G1/S progression contribute to cell-cycle arrest in the intestine and M lineage. Inactivation of *lin-35* by RNAi or putative null mutation (*n745*) combined with *fzr-1* loss of function results in a larval lethal and sterile phenotype, with extra cell divisions in multiple lineages (Fay et al., 2002). For lineage-specific loss of function, we placed a *fzr-1* genomic fragment in the reporter plasmid (Figure 1A). Mos1-mediated single-copy insertion (MosSCI) of this plasmid rescued the *fzr-1(ku298)* strong loss-of-function mutation, as it restored viability, fertility, and cell-cycle exit in *lin-35(RNAi* or *n745);fzr-1(ku298)* double mutant larvae (Figures 2C and 3A). For simplicity, we use *fzr-1^{lox}* to indicate the combination of *fzr-1^{lox}* transgene and *fzr-1(ku298)* allele (Table S7 lists complete genotypes of all strains). Intestine-specific CRE expression (*Pelt-2::CRE*) in *lin-35(RNAi);fzr-1^{lox}* animals caused extra division of intestinal nuclei, similar to the extra intestinal divisions in *lin-35(RNAi);fzr-1(ku298)* larvae (Figure 2C; Table S3). In contrast to the latter, however, *lin-35(RNAi)* animals with CRE-induced *fzr-1* loss were fully fertile and viable. Thus, validating our system, *Pelt-2::CRE* expression induced intestine-specific *fzr-1* inactivation while leaving other tissues unaffected.

Remarkably, examination of the M lineage revealed that *lin*-35 Rb and *fzr-1* are not critical for cell division control in this lineage. Use of the *readout^{lox}* reporter helped determine that *lin-35(RNAi* or *n745);fzr-1(ku298)* double mutants undergo normal temporal arrest of SM cell division and cell-cycle exit during terminal differentiation (Figure 2D; Table S4). Not surprisingly, lineage-specific loss of *fzr-1^{lox}* combined with *lin-35* inactivation also did not alter the cell division and differentiation pattern in the postembryonic mesoderm lineage (Figure 2D; Table S4). Thus, *lin-35* Rb and *fzr-1* show lineage-dependent requirements, and other cell-cycle regulators are sufficient for temporal and permanent cell-cycle arrest in the M lineage.

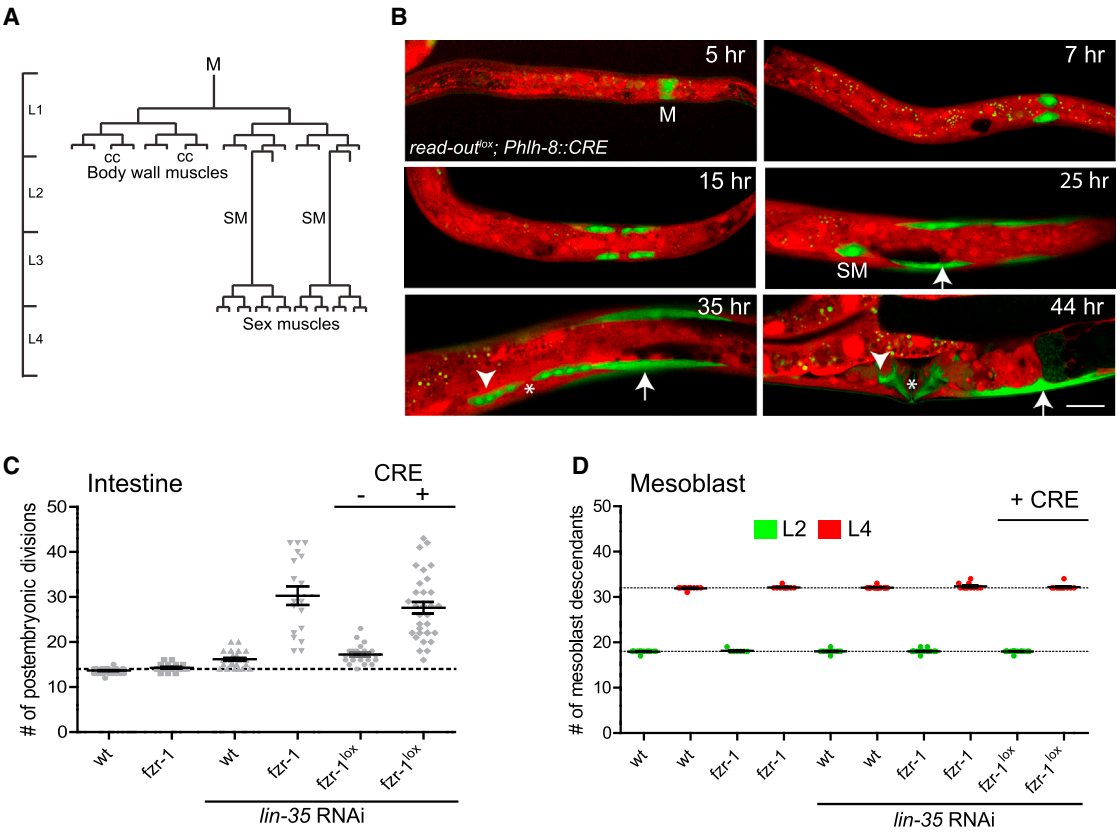

Figure 2. Lineage-Specific Requirement for *lin-35* Rb and *fzr-1* FZR1/Cdh1 in Cell-Cycle Arrest

(A) Mesoblast (M) lineage and division pattern in the hermaphrodite. Cell divisions generate 18 M daughter cells in the L1 stage. 16 of these cells differentiate into body-wall muscle cells and coelomocytes (CC). Two sex myoblasts (SM) migrate anteriorly and divide again in the third larval stage to form muscles required for egg laying.

(B) Fluorescence microscopy images of mesoblast descendants (eGFP positive, green), visualized by CRE-loxP based recombination of the *readout*^{lox} reporter (Figure 1) following *Phlh-8::CRE* expression. Arrows: differentiated body-wall muscle. Arrowheads: daughter cells from the SM, *Position of the vulva. Scale bar, 20 μm.

(C and D) Comparison between a homozygous *fzr-1(ku298)* strong loss-of-function mutant and lineage-specific *fzr-1*^{lox} knockout. (C) Number of postembryonic nuclear divisions in the intestine upon inactivation of *fzr-1* alone or *fzr-1* and *lin-35*. (D) Number of mesoblast descendants upon inactivation of *fzr-1,* or *fzr-1* and *lin-35,* in L2 and L4. Graphs show mean ± SEM; each dot represents a single animal; the dotted line indicates the average number in wild-type (WT).

See also Tables S3 and S4.

Reliable Cell-Cycle Arrest through Multiple Levels of Control

To identify regulators that control temporal cell-cycle exit in muscle precursor cells, we performed a candidate-based RNAi screen. This included all genes with a reported cell-cycle inhibitory function in *C. elegans* as well as transcription factors and chromatin modifiers with a potential contribution in cell-cycle arrest (Table S5). Gene knockdown by feeding RNAi was tested in parallel in the M-lineage reporter strain (*readout*^{lox}*;Phlh-8::CRE*) and in M-lineage double mutant animals *lin-35(n745);fzr-1*^{lox}*;Phlh-8::CRE* (Table S4). We identified six genes that when singly inactivated by RNAi interfered with M-lineage cell-cycle exit in the readout control strain. These genes encode the well-known *C. elegans* CDK inhibitor CKI-1 Kip1, and two SCF-like E3 ubiquitin ligase subunits, CUL-1 and LIN-23 β-TrCP (Figure 3A; Figure S3; Table S4; quantified for sex muscles). In addition, inhibition of three subunits of the SWI/SNF chromatin-remodeling complex allowed extra divisions in the M lineage (Figures 3A and S3; Table S4). Thus, the function of each of these genes is critical for correct cell-cycle exit in the mesoblast lineage. At the same time, differentiated muscle cells were still formed following knockdown of these genes, and the number of sex muscles at most doubled (Figure 3A).

When tested in combination, the different levels of control were found to act partly redundantly in promoting cell-cycle exit. Even though the parental strain *lin-35(n745); fzr-1*^{lox}*;Phlh-8::CRE* showed a normal M-lineage division pattern, the presence of *lin-35* and *fzr-1* single or double mutations substantially increased the numbers of M descendants when combined with RNAi of either *cki-1* Kip1, *lin-23* β-TrCP, *cul-1* Cullin1, or the SWI/SNF genes *swsn-1* BAF155/170, *swsn-5* (*snfc-5*) SNF5/INI1, and *swsn-2.1* BAF60 (Figures 3A and S2; Table S4). Specifically, when combined with *cki-1(RNAi)*, the *lin-35(n745)* and *fzr-1(ku298)* single mutations significantly

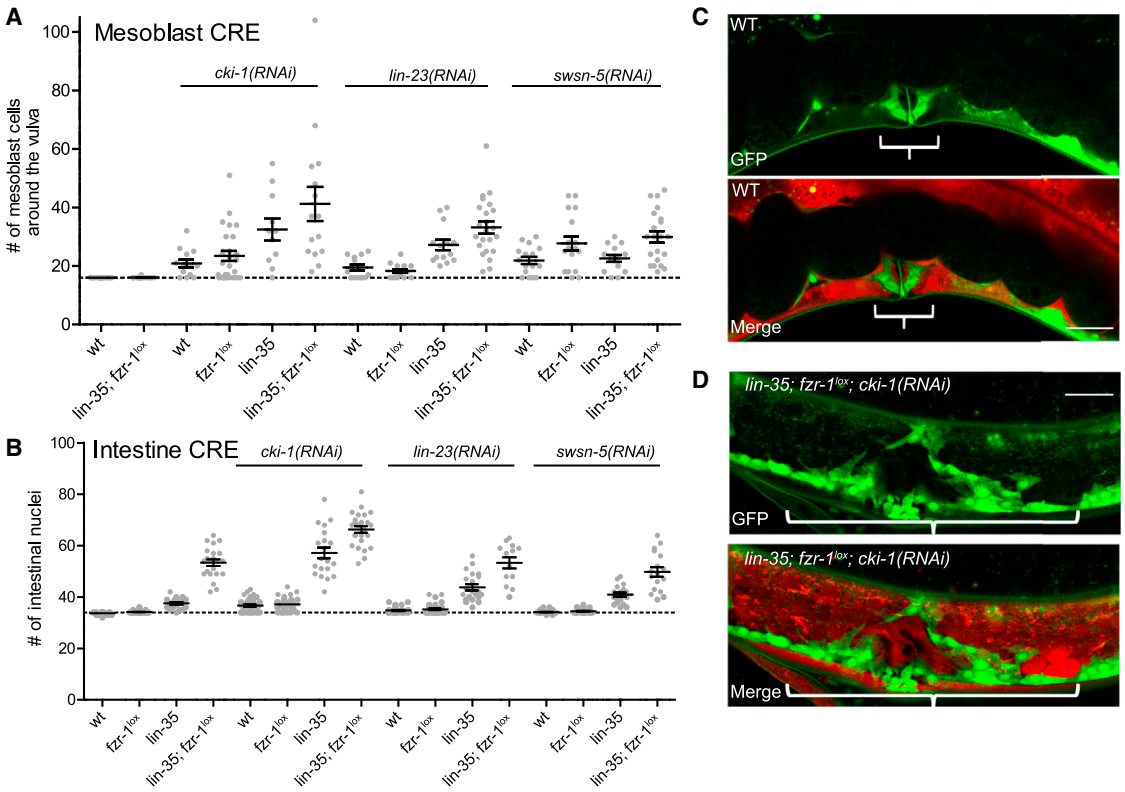

Figure 3. Cooperative Control of Cell-Cycle Exit by G1/S Inhibitors and SWI/SNF Subunits

(A–D) RNAi of the indicated genes combined with *lin-35*-null mutation and lineage-specific *fzr-1* knockout.

(A) Quantification of the number of mesoblast descendants localized around the vulva for the indicated genotypes.

(B) Quantification of the number of intestinal nuclei for the indicated genotypes. Graphs show mean ± SEM. Each dot represents a single animal; the dotted line indicates the average numbers in WT.

(C and D) Fluorescence microscopy images of mesoblast descendants (eGFP positive). Bracket indicates vulva region. (C) *readout^{lox};Phlh-8::CRE* control animal with 16 sex muscles. (D) Illustration of animal with a substantial over-proliferation phenotype, following RNAi of *cki-1* in *lin-35(n745);fzr-1^{lox};Phlh-8::CRE* larvae. Scale bars represent 20 μm. See also Figure S3, Tables S3, S4, S5, and S6.

enhanced the number of M descendants around the vulva, and the triple gene inactivation resulted in further increased numbers of cell division (Figures 3A, 3C, 3D, and S3; Table S4). Similarly, the *lin-23* RNAi phenotype was significantly stronger in *lin-35* single mutants, while the strongest effects were observed in *lin-35;fzr-1^{lox};hlh-8::CRE* mutants. Hyperplasia of vulval muscles induced by RNAi of SWI/SNF genes was enhanced by *fzr-1* mutation in the mesoblast lineage (Figures 3A and S3; Table S4). While the effect of *lin-35* mutation could possibly arise from enhanced RNAi (Wang et al., 2005), this is not the case for *fzr-1* loss.

Comparing the results in the M lineage to the intestine, lineage-dependent differences were observed again. Only *cki-1* RNAi further increased the number of nuclear divisions in the intestine of *lin-35(n745);fzr-1^{lox};Pelt-2::CRE* double mutants (Figures 3B and S3; Table S3). RNAi of *lin-23* and *cul-1* increased the number of divisions of intestinal nuclei in *lin-35(n745)* single-mutant larvae. By contrast, inactivation of SWI/SNF subunits did not affect the number of divisions in the intestine (Figures 3B and S3; see Discussion). While the relative contribution of each regulator varies between cell lineages, these results show that multiple levels of control act in cooperation to arrest the cell cycle both in the intestine and mesoblast lineage.

G1/S Inhibitors Act Largely Redundantly with the SWI/SNF Complex in Cell-Cycle Exit

To better define SWI/SNF contribution in cell-cycle control, we examined additional mutant combinations. SWI/SNF components form highly conserved chromatin remodeling complexes that use ATPase activity to remodel nucleosome positions, thereby increasing or reducing access to transcriptional regulators (reviewed in Wilson and Roberts, 2011). The complexes contain several core subunits, including an ATPase subunit known as Brahma (BRM) in *Drosophila*, human BRM (hBRM) and BRM-Related Gene 1 (BRG1), and SWSN-4 in *C. elegans*. BRM/BRG1-associated factors (BAFs) include other core subunits (*swsn-1* BAF155/170 and *swsn-5* BAF47/SNF5/INI1 in *C. elegans*), as well as additional accessory and signature subunits (Table S6) (Riedel et al., 2013; Sawa et al., 2000; Shibata et al., 2012). Based on signature subunit composition, two different complexes, BAF and PBAF, have been distinguished. While *swsn-4* was not present in our RNAi libraries, the other

SWI/SNF core subunits *swsn-1* and *swsn-5*, as well as the accessory subunit *swsn-2.1* (BAF60/SMARCD3), were found to induce extra M-lineage divisions in our screen (Figure S3; Table S5). RNAi for three different PBAF-specific components (*pbrm-1* BAF180/Polybromo, *swsn-7* BAF200/ARID2, *swsn-9* BRD7) did not result in a cell division phenotype (Table S5). Thus, SWI/SNF activity, and possibly specifically a *C. elegans* BAF-related complex, appears to contribute to cell-cycle arrest.

As loss of SWI/SNF-complex function is incompatible with viability, we created lineage-specific knockout strains for further analysis. For technical reasons, we focused on the *swsn-1(os22)* temperature-sensitive allele, which causes strong loss of function at the non-permissive temperature of 25°C, while being viable at 15°C (Supplemental Experimental Procedures). Similar to the effect of *swsn-5* RNAi, shift of *swsn-1^{lox};Phlh-8::CRE* embryos from 15 to 25°C increased the number of M descendants (Figure 4A; Figure S3; note that *swsn-1^{lox}* refers to the combined *swsn-1(os22)* mutation and *swsn-1^{lox}* single-copy rescuing transgene). Combining *swsn-1* inactivation with single *lin-35*, *cki-1*, or *fzr-1* mutation or RNAi further increased the number of M descendants (Figure 4A). Remarkably, lineage-specific inactivation of *swsn-1* combined with RNAi of either *cul-1* or *lin-23* resulted in a massive increase in M-lineage descendants, which was further enhanced by *fzr-1* inactivation (Figures 4B and 4C; Figure S4; Table S4). Similarly, *swsn-1^{lox};Phlh-8::CRE* combined with *lin-35(n745)* and *cki-1(RNAi)* resulted in a dramatic over-proliferation phenotype, which was even stronger when combined with *fzr-1^{lox}* (Figures 4B, 4D, and S4; Table S4). While the use of non-null alleles may contribute to this enhanced effect, the limited over-proliferation observed after severe knockdown of individual SWI/SNF genes or G1/S inhibitors stood in stark contrast with the phenotype of combined mutants (Figures 2, 3, and 4). Even double or triple loss of function of the canonical G1/S inhibitors caused limited defects, which were greatly enhanced by simultaneous *swsn-1* inhibition. These results demonstrate that the SWI/SNF complex and G1/S inhibitors provide substantially overlapping contributions in promoting cell-cycle exit.

Tumorous Over-Proliferation of Somatic Cells in *C. elegans*

Several additional observations confirm that the combined inactivation of *swsn-1* and previously characterized G1 regulators causes uncontrolled cell proliferation and a tumorous phenotype. First, to examine whether individual cells or large multinucleated cells are formed, we dissected *lin-23(RNAi);swsn-1^{lox};Phlh-8::CRE* animals in iso-osmotic medium. Upon cutting the cuticle, cells streamed from the carcass, including many individual green fluorescent cells (Figure 4E). Addition of DAPI did not result in DNA staining of these eGFP-positive cells in iso-osmotic medium, while DAPI staining of fixed animals indicates a normal DNA content of the eGFP positive cells (Figure 4G; data not shown). This indicates that the M-lineage descendants contain an intact plasma membrane. Thus, the combined loss of *swsn-1* and G1/S inhibitors leads to the formation of many extra individual cells.

To further characterize the phenotype, we performed live observations of single animals by combined immunofluorescence and differential interference contrast (DIC) microscopy. We observed increased numbers of M descendant cells in the early L2 stage, but not before completion of the L1 division pattern (Figure 4F). We followed M-lineage divisions in four individual *fzr-1^{lox};swsn-1^{lox};lin-23(RNAi);Phlh-8::CRE* animals from the moment that eight daughter cells are formed. In all four animals, apparently normal cell divisions continued in the M lineage, which resulted in the generation of 18 daughter cells at normal positions (Figures 2A and 2B). Mutant animals synchronized by developmental staging all showed 8 to 18 M-derived cells at 12 hr of larval development. In the large majority (22 of 24) of these larvae, the pattern of M descendants was normal, while two showed abnormal positioning of M daughters, but no extra cells. Following the 18-cell stage, divisions in the M lineage continued in four out of five mutants, while the corresponding cells in wild-type animals undergo prolonged cell-cycle arrest (Figure 4F). Extra divisions were observed in every quadrant, with continued proliferation of daughter cells that normally become post-mitotic and initiate terminal differentiation at this stage.

We examined incorporation of the thymidine analog EdU to visualize DNA synthesis. Combined detection of EdU and immunohistochemical staining of eGFP demonstrated continued DNA synthesis in M daughters of lineage-specific *swsn-1* knockdown, *lin-23(RNAi)* larvae (Figure 4G). Quantification of cell numbers by counting the eGFP-positive cells indicated that the number of M descendants increased substantially during the L2 stage, and also during the L3 and L4 stages (Figure 4B). These numbers approximately doubled again during a 24 hr time span of development from L4 into the adult stage, at which time no somatic cell division takes place in the wild-type (Figure 4B). Reduced viability and cell disintegration prevented counting at later time points. Amazingly, some young adults contained well over 300 M-lineage cells, formed from a single precursor in three days time and corresponding to approximately a third of the somatic cells in a normal adult animal. Together, these data show that combined loss of *swsn-1* and G1/S inhibitors results in tumorous over-proliferation in the *C. elegans* soma.

The SWI/SNF Complex Cooperates with *hlh-1* MyoD in Cell-Cycle Exit

In contrast to the G1/S inhibitors, a function of the SWI/SNF complex in cell-cycle exit is poorly defined. Previous chromatin immunoprecipitation (ChIP) experiments identified several thousand *C. elegans* genes associated with SWI/SNF subunits (Riedel et al., 2013). Examining the available chromatin immunoprecipitation (ChIP) data of SWSN-1::GFP and SWSN-4::GFP (Riedel et al., 2013), we observed SWI/SNF promoter occupancy at eight out of nine negative regulators of cell-cycle progression, and three out of eight positive regulators (Figure S5). SWI/SNF-dependent chromatin remodeling is particularly important for the coordinated switching of gene expression programs during lineage commitment (Eroglu et al., 2014; Wilson and Roberts, 2011). As human MyoD acts in concert with SWI/SNF components (Puri and Mercola, 2012; de la Serna et al., 2001), the *C. elegans* SWI/SNF complex may act together with the myogenic transcription factors of the M lineage, in particular, HLH-1 MyoD. Chromatin association of HLH-1 MyoD has been

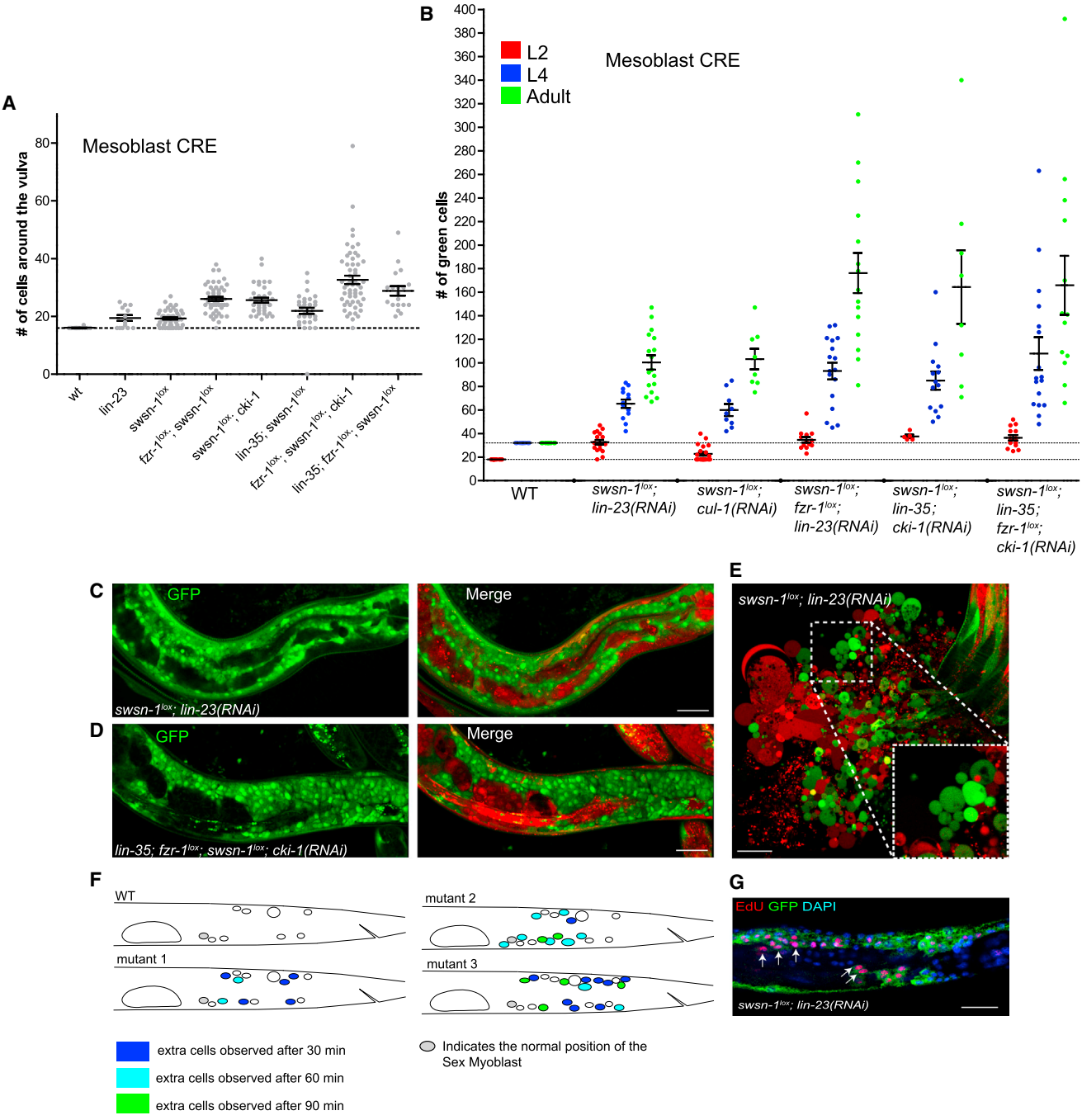

Figure 4. Combined Inactivation of *swsn-1* with G1/S Inhibitors Leads to Dramatically Increased Proliferation in the Mesoblast Lineage

(A and B) RNAi of the indicated genes combined with *lin-35(n745)*-null mutation and lineage-specific inactivation of *swsn-1* and *fzr-1*. (A) Quantification of the number of mesoblast descendants localized around the vulva. (B) Quantification of the total number of mesoblast descendants of the indicated genotypes in L2 (red), L4 (blue), and adult (green). Graphs show mean ± SEM; each dot represents a single animal; dotted lines in the graphs indicate average WT number.

(C and D) Representative fluorescent images of mesoblast over-proliferation (green, eGFP positive) in animals of indicated mutant genotypes.

(E) Fluorescence microscopy image of cells following dissection of animals as in (D) in iso-osmotic medium.

(F) Graphical illustrations of lineage analysis of proliferation patterns in young *fzr-1^{lox}; swsn-1^{lox}; lin-23(RNAi)* animals, based on combined immunofluorescence and DIC microscopy. Animals containing 18 posterior myoblast daughter cells (as in WT) were imaged every 30 min to follow the initial steps of the over-proliferation phenotype. Only the left half of the animals, with nine M-daughter cells, are shown in the cartoons. Dark blue, light blue, and green circles: cells formed during the first 30 min of imaging, between 30 and 60 min, or between 60 and 90 min after the start of the experiment, respectively. Gray cell indicates the initial SM.

(G) Incorporation of EdU (red) in mutant M descendants (green) during L2–L4 development. Nuclei are marked with DAPI (blue).

Scale bars, 20 μm. See also Figure S4 and Tables S3 and S4.

extensively characterized in previous experiments (Boyle et al., 2014; Lei et al., 2010). Visual inspection of promoter regions showed strong overlap between SWI/SNF and HLH-1 occupancy, not only at muscle-specific genes (e.g., *myo-3* myosin), but also at several positive (*cdk-4, cye-1)* and negative *(cki-1, cki-2, cdc-14)* G1 regulatory genes (Figure S6). Using a temperature sensitive *hlh-1* MyoD allele, we observed that partial *hlh-1* loss of function at 25°C resulted in increased numbers of M descendants around the vulva, to a similar extent as *hlh-1, swsn-1* double mutants (Figure 5A; Table S4). While this supports a concerted function, the *hlh-1(cc561*ts*)* phenotype resulted largely from SM duplication, whereas extra M-lineage divisions following *swsn-1* loss appeared more random (Figure 4F). When combined with *lin-23* RNAi, the *hlh-1* mutation caused severe over-proliferation to a similar degree as mesoblast-specific *swsn-1* inactivation (Figure 5B; Table S4). Combining *hlh-1(cc561*ts*)* and *swsn-1* knockout with *lin-23(RNAi)* further increased M-lineage proliferation, which may reflect incomplete loss of function or point to partially non-overlapping contributions of *hlh-1* and *swsn-1*. Nevertheless, the substantial overlap in over-proliferation phenotypes indicates that SWI/SNF and HLH-1 MyoD act together to induce cell-cycle arrest in the transition of proliferating precursor cells to differentiated post-mitotic muscle cells.

SWI/SNF Antagonizes PcG Gene Function and Controls Positive and Negative Cell-Cycle Regulators

SWI/SNF chromatin remodeling has been proposed to antagonize transcriptional repression by Polycomb group (PcG) proteins. *C. elegans* uses a protein complex of MES-2, MES-3 and MES-6 with similarity to the Polycomb Repressive Complex 2 (PRC2) (Gaydos et al., 2012). We observed that RNAi of the PcG-related genes *mes-2* EZH2 and *mes-3* significantly suppressed over-proliferation induced by *swsn-1* mutation or *fzr-1, swsn-1* double mutation (Figure 5C; Table S4). Thus, the over-proliferation phenotype may result from PcG-mediated repression of genes that normally are SWI/SNF-dependently induced during muscle differentiation.

When combined with M-lineage-specific *fzr-1* and *swsn-1* inactivation, strong RNAi of *mes-2* EZH2 or *mes-3* reduced the extra divisions only in part (Figure 5C). As loss of *fzr-1* alone does not alter the M lineage, these observations appear to indicate that SWI/SNF also has functions unrelated to antagonizing PcG. *C. elegans* SWI/SNF proteins occupy promoters of positive as well as negative regulators of cell division (Figure S5; Riedel et al., 2013). Hence, the SWI/SNF complex could stimulate cell-cycle exit through transcriptional activation of G1/S inhibitors, and in addition through transcriptional silencing of cell-cycle entry promoting genes such as *cye-1* Cyclin E. To examine this possibility, we created a *cye-1* transcriptional reporter. This *Pcye-1::tagBFP* reporter was expressed in post-mitotic M-derived muscle cells of lineage-specific *swsn-1* mutants, in contrast to the corresponding cells in wild-type control animals (Figures 5D and 5E). These data support SWI/SNF-mediated transcriptional repression of *cye-1* cyclin E during cell-cycle withdrawal.

To extend these observations, we performed single-molecule FISH (smFISH) experiments for positive (*cye-1, cdk-4*) and negative (*cki-1, cdc-14*) cell-cycle regulators identified as potentially SWI/SNF and HLH-1-regulated genes (Figure S6). We also included *myo-3* myosin as an example of a probable SWI/SNF and HLH-1 MyoD-regulated muscle-specific gene (Figure S6). *cyd-1* Cyclin D was not identified as a SWI/SNF target in previous ChIP experiments and served as a control (Figure S5; Riedel et al., 2013). Simultaneous smFISH labeling with anti-eGFP probes helped visualize the M-derived muscle cells in *readout^{lox}*; *Phlh-8::CRE* control animals and *swsn-1^{lox};Phlh-8:CRE* mutants (Figure 5F).

We detected *cye-1* and *cdk-4* mRNA expression in post-mitotic muscle cells of M-lineage-specific *swsn-1* mutants (Figure 5G). The corresponding muscle cells in control animals basically did not express *cye-1* mRNA, and showed significantly fewer *cdk-4* mRNA molecules. Conversely, the numbers of *cki-1*, *cdc-14*, and *myo-3* mRNA molecules in M-lineage muscle cell were substantially reduced in *swsn-1* mutants, compared to wild-type controls (Figures 5G and 5H). Neither the control nor *swsn-1* mutants expressed *cyd-1* mRNA in arrested M-lineage muscle cells (Figure 5G). Thus, only the G1/S regulator genes with a SWI/SNF-occupied promoter showed significantly induced (*cye-1* and *cdk-4*) or reduced (*cki-1* and *cdc-14*) expression following *swsn-1* inactivation. Importantly, the *cye-1* transcript numbers further increased when the *swsn-1* mutation was combined with a *lin-35(n745)* mutation (Figure 5G). This observation lends support for independent yet cooperative functions of SWI/SNF and *lin-35* Rb complexes in *cye-1* cyclin E repression. Together, these results support that the SWI/SNF complex contributes to both positive and negative regulation of cell-cycle gene expression during muscle differentiation.

Combined G1/S Inhibitor and SWI/SNF Loss Leads to Continued Proliferation of Muscle Precursors

The over-proliferating cells could remain present as undifferentiated precursor cells, could become highly undifferentiated, or could obtain an in-between or random fate. To distinguish between these possibilities, we examined several markers for M-lineage descendants. The HLH-8 Twist transcription factor is expressed in undifferentiated precursor cells of the M lineage, but not in the differentiated muscle cells and coelomocytes (Corsi et al., 2000). We examined expression of a *Phlh-8::tagBFP* transcriptional reporter in the *readout^{lox}* strain and two M-lineage mutant strains (Figures 6A–6C). Expression of tagBFP was apparent in all precursor cells of the M lineage, including the migrating sex myoblasts (SM). However, at the time of muscle differentiation, tagBFP expression disappeared (Figure 6A). In *swsn-1* M-lineage knockout mutants treated with *lin*-23 RNAi, approximately half of the daughter cells maintained *Phlh-8-8::tagBFP* expression, even at late larval stages. This number increased considerably when *swsn-1 lin*-23 double inactivation was combined with *fzr-1* loss (49.8% versus 81.7% tagBFP-positive M descendants in the double versus triple mutant, respectively; Figures 6B and 6C; Figure S7). Thus, increased proliferation in the M lineage correlated with a higher percentage of M descendants maintaining expression of the *hlh-8* Twist precursor cell reporter.

We also examined actin and UNC-15 paramyosin expression and organization, as markers for muscle differentiation. As

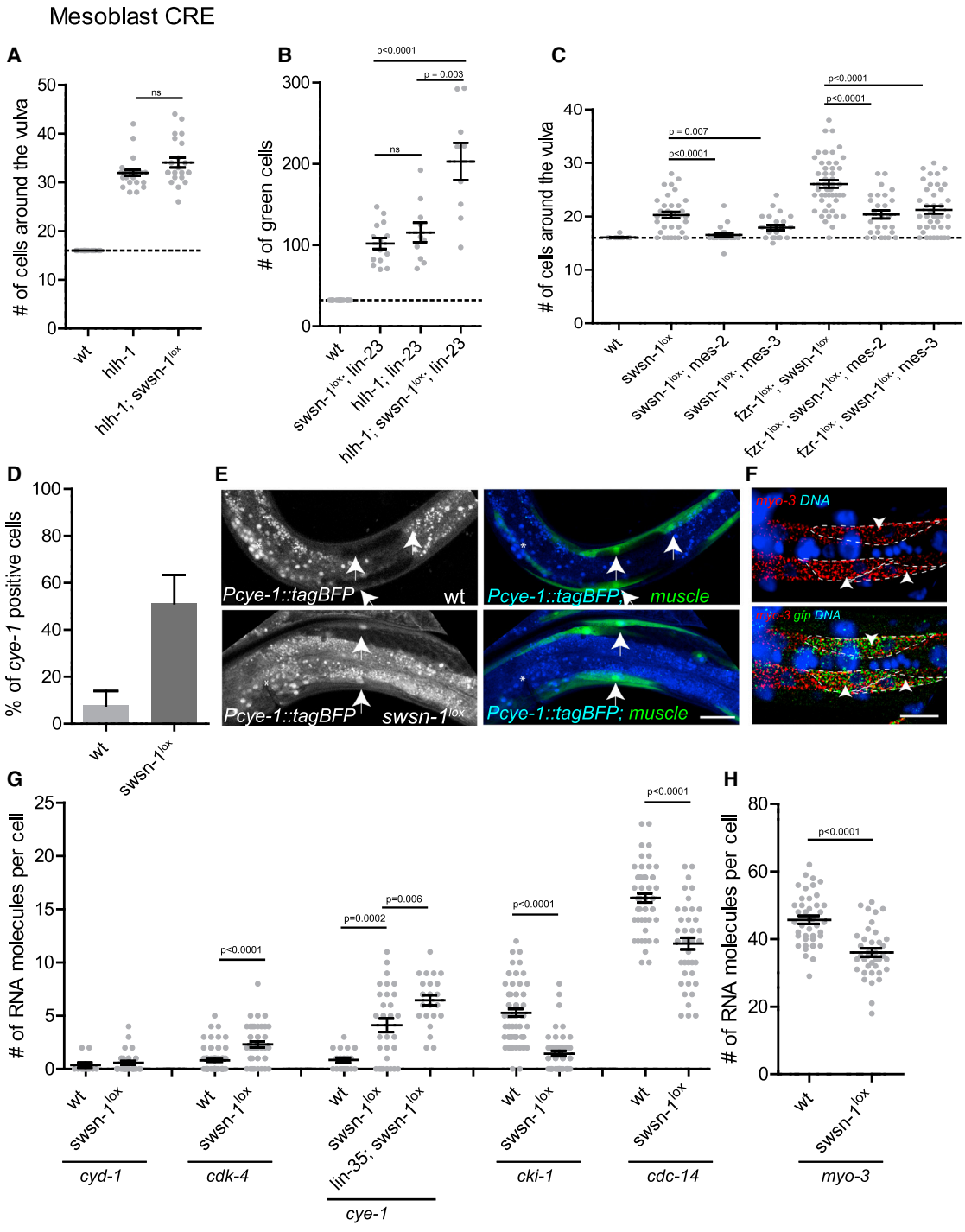

Figure 5. Control of Cell-Cycle Arrest and Differentiation by SWI/SNF Chromatin Remodeling

(A and B) Quantification of the number of mesoblast descendants in wild-type and *hlh-1(cc561ts)* animals at the non-permissive temperature, combined with lineage-specific inactivation of *swsn-1* (A) and/or *lin-23* RNAi (B).

(C) Quantification of mesoblast descendants around the vulva in *swsn-1* or *fzr-1; swsn-1* mutants in combination with *mes-2* EZH2 or *mes-3* RNAi.

(D) Quantification of the percentage post-mitotic muscle cells expressing *Pcye-1::tagBFP* in WT and mutants with M-lineage-specific *swsn-1* inactivation.

(E) Representative fluorescence microscopy images of animals quantified in (D).

(F) smFISH staining using Cy5-labeled probes for *myo-3* and TMR-labeled probes for GFP.

(legend continued on next page)

visualized by immunohistochemical analysis, the eGFP-positive M-lineage-derived body-wall muscle cells intercalated with the embryonic body muscles and formed well-organized myofilaments (Figures 6D and 6F, top). The eGFP positive M descendants in *lin-23(RNAi) fzr-1^{lox};swsn-1^{lox};Phlh-8::CRE* mutants rarely showed organized myofilaments, and the majority did not show detectable actin or UNC-15 paramyosin expression (Figures 6D–6G and S7). However, muscle markers were expressed in some cells, and the percentage of actin or paramyosin expressing cells was substantially higher in *lin-23(RNAi);swsn-1^{lox};Phlh-8::CRE* mutants with wild-type *fzr-1*, compared to mutants that also lacked *fzr-1* function. This is consistent with the proliferating M-lineage cells either maintaining progenitor status or initiating incomplete muscle differentiation. These observations highlight the inverse regulation of cell proliferation and differentiation.

DISCUSSION

Our experiments based on CRE-lox mediated recombination and lineage tracing uncovered tissue-type-specific regulatory mechanisms for cell division arrest that cause tumorous over-proliferation of somatic cells when deregulated in *C. elegans*. We found five distinct levels of control to contribute to cell-cycle exit: CDK inhibitory protein expression, LIN-35 Rb-mediated transcriptional repression, APC/C^{FZR-1} and SCF^{LIN-23} catalyzed protein degradation, and SWI/SNF-mediated chromatin remodeling. These controls appear largely redundant and partly additive, together creating a highly robust decision to exit the cell division cycle. The contribution of SWI/SNF mediated chromatin remodeling is critical, as excessive over-proliferation occurred only when inactivation of G1/S inhibitors was combined with SWI/SNF gene loss. Our data together with the described molecular functions support a model in which the different G1/S inhibitors and SWI/SNF complex provide alternative mechanisms to block the cell-cycle machinery, converging at the CDK-4/Cyclin D and CDK-2/Cyclin E kinases and initiation of DNA synthesis (Figure 7).

The cell-cycle arrest network is complex, because the regulators involved act redundantly, have multiple substrates, and provide feedback control. The Rb/E2F and SWI/SNF complexes affect the transcription of many genes, and the APC/C^{FZR1} and SCF^{LIN-23} E3 ligases target multiple proteins for degradation. Nevertheless, a limited number of regulatory steps may be crucial for cell-cycle exit. We found LIN-35 Rb and SWI/SNF to converge on *cye-1* Cyclin E transcriptional repression, while CKI-1 likely blocks CDK-2/CYE-1 Cyclin E kinase activity. Moreover, CUL-1 and LIN-23 β-TrCP have been implicated in G1 cyclin protein degradation (Kipreos et al., 1996, 2000), while experimental evidence points to SCF^{LIN-23} catalyzed degradation of the CDK-cyclin activating phosphatase CDC-25.1 (Hebeisen and Roy, 2008). Targets of the APC/C^{FZR-1} are currently not known in *C. elegans.* Our recent results indicate that FZR-1 and LIN-35 pRb are the most critical substrates of CDK-4/cyclin D kinases (The et al., 2015). As such, combined loss of *lin-35* Rb and *fzr-1* alleviates cell-cycle arrest by bypassing the requirement for CDK-4/cyclin D kinase activity. Mesoblast descendants do not continue proliferation in *lin-35* Rb, *fzr-1* double mutants, which likely reflects requirement for CDK-2/Cyclin E activation for S phase initiation. In the double mutants, CDK-2/Cyclin E activity is still inhibited through CKI-1 Kip1 association, SCF^{LIN-23}-induced degradation of CDC-25.1, and SWI/SNF-dependent cyclin E transcriptional repression. Such alternative and partly non-overlapping levels of G1 CDK-cyclin inhibition can explain the observed genetic interactions between the different regulators (Figure 7).

SWI/SNF chromatin remodeling complexes act as global regulators of transcription. *Drosophila* SWI/SNF genes were identified as TrxG members with a positive role in Homeotic (HOX) gene expression or antagonism of PcG-mediated silencing (Schuettengruber et al., 2011). Suppression of the *swsn-1* over-proliferation phenotype by PcG-related gene knockdown indicates that the antagonism between SWI/SNF and PcG gene function is conserved in *C. elegans.* Re-introduction of human SNF5 (BAF47/INI1) in SNF5 mutant rhabdoid tumor cells was found to induce PcG complex removal, transcription of the p16^{INK4A} and p21^{CIP1} genes, and cell proliferation arrest (Chai et al., 2005; Kia et al., 2008; Kuwahara et al., 2013). Similarly, our results could be explained by PcG-mediated silencing of G1/S inhibitor genes that are normally activated by the SWI/SNF complex. However, this cannot explain the enhanced expression of positive cell-cycle regulators in the *swsn-1* mutant. Transcriptional suppression by SWI/SNF-mediated chromatin remodeling could indirectly result from an induced factor, as has recently been described in *Drosophila* neural stem cells (Eroglu et al., 2014). In contrast, our data, based on SWI/SNF promoter occupancy combined with reporter expression and smFISH experiments, support a direct contribution of SWI/SNF-mediated chromatin remodeling in transcriptional repression of *cye-1* and *cdk-4*. Together, these data are consistent with the model that SWI/SNF-mediated chromatin remodeling antagonizes PcG and promotes transcription of negative cell-cycle regulators during differentiation, while simultaneously acting in cooperation with pRb to repress the transcription of positive regulators.

We found SWI/SNF gene function to be crucial for cell-cycle arrest in the mesoblast lineage, but not in the intestine. Notably, differentiated embryonic intestinal cells do not exit the cell cycle as they continue nuclear divisions and rounds of DNA synthesis during larval development (Hedgecock and White, 1985). In contrast, cells in the M-lineage transition from proliferating precursors to terminally differentiated post-mitotic cells (Sulston and Horvitz, 1977). This transition combines cell-cycle withdrawal with activation of a muscle-specific

(G and H) Detection of cell-cycle and muscle-specific gene transcripts using smFISH, showing the number of fluorescent spots corresponding to the indicated mRNAs in post-mitotic muscle cells of the indicated genotypes.

Arrows indicate differentiated M-lineage muscles (green). Graphs show mean ± SEM; each dot represents a single animal (A–C) or single cell (G and H). Dotted lines (A–C) indicate average WT numbers. Scale bars, 20 μm in (E) and 5 μm in (F). See also Figures S5 and S6 and Tables S3 and S4.

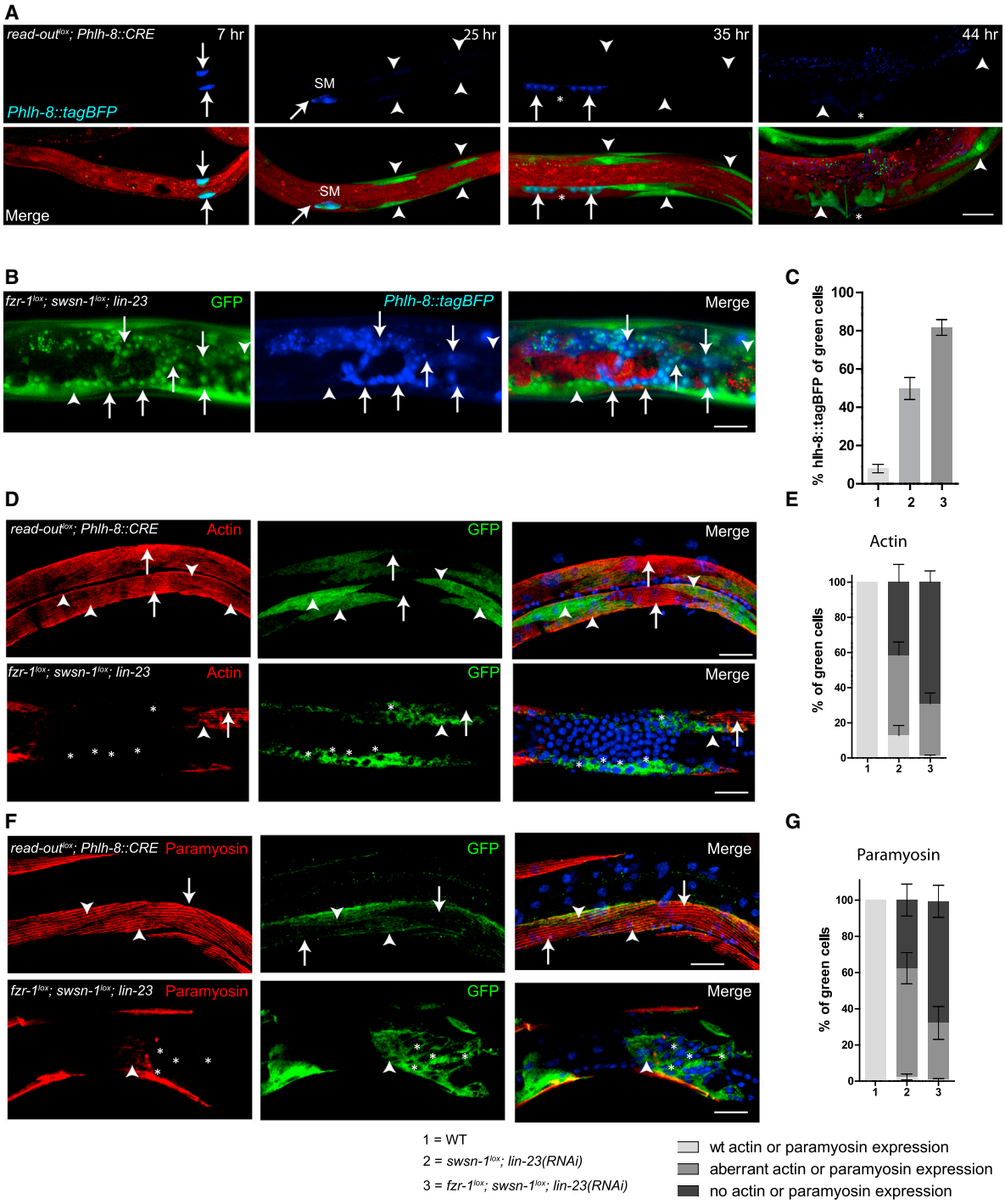

Figure 6. Limited Differentiation of Over-Proliferating Mesoblast Descendants

(A and B) Fluorescence microscopy images showing *hlh-8* Twist promoter activity (tagBFP, Blue) in M-daughter cells (eGFP-positive, green). (A) Wild-type control, tagBFP is visible in precursor cells (arrows), but not in differentiated muscle cells (arrowheads). Asterisks (*) indicate the position of the vulva. (B) *fzr-1^{lox}; swsn-1^{lox}; lin-23(RNAi)* mesoblast mutant. M-derived cells with *Phlh-8::tagBFP* expression are indicated by arrows, without *Phlh-8::tagBFP* expression with a arrowhead.

(C) Percentage of green cells positive for *Phlh-8::tagBFP* in animals of the indicated genotypes (bottom).

(D and F) Staining of muscle differentiation markers, actin (red) (D), and paramyosin (red) (F) in L4 wild-type and mutant larvae. GFP: mesoblast descendants are visualized by anti-GFP antibody staining (green), nuclei by DNA staining (DAPI, blue). Arrows indicate non-mesoblast-derived differentiated muscle cells (GFP

(legend continued on next page)

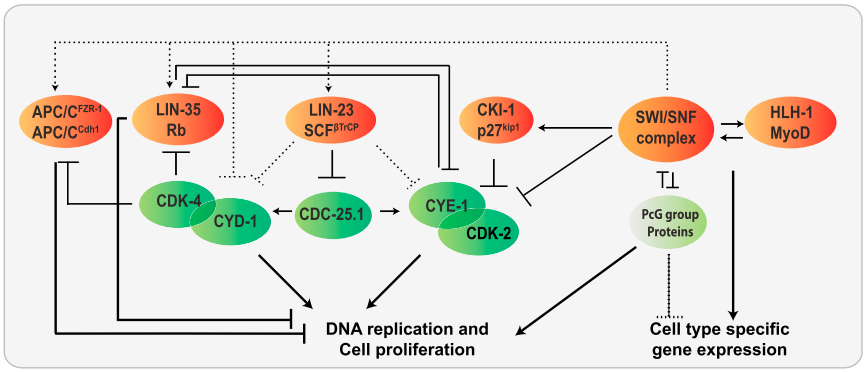

Figure 7. Model for Developmental Arrest of Cell Division

Ub-dependent protein degradation, Rb-mediated transcriptional repression, and association of CDK-inhibitory proteins with CDK/cyclin complexes promote cell-cycle arrest. During terminal differentiation, SWI/SNF complexes in cooperation with lineage-specific transcription factors provide an additional level of control. The different G1/S inhibitors and SWI/SNF complex cooperate by providing alternative levels of control over the basic cell-cycle regulators, with each level antagonizing CDK-4/CYD-1 cyclin D and/or CDK-2/CYE-1 cyclin E kinase activity. Together, these regulators provide a highly robust control network for cell-cycle exit. See also Figures S5 and S6.

gene expression program. Previous studies of differentiating myoblasts implicated SWI/SNF-mediated chromatin remodeling in muscle-specific gene expression (Puri and Mercola, 2012; de la Serna et al., 2001). This activation of cell-type-specific gene expression likely coincides with SWI/SNF-mediated chromatin remodeling at cell-cycle gene promoters (see above; Figure 7). Transcriptional activation and inactivation of cell-cycle genes by the SWI/SNF complex provides a mechanism for cell-cycle exit that may be employed specifically during terminal differentiation, and which still can be effective when multiple G1/S inhibitors are lost. This could be the main difference between permanent cell-cycle arrest and temporary quiescence.

Recent cancer genome sequencing studies and identification of additional SWI/SNF accessory and signature factors have revealed that inactivation of SWI/SNF components occurs in a broad spectrum of human cancers, at an astonishing average frequency of nearly 20% (Kadoch et al., 2013; Kandoth et al., 2013; Wang et al., 2014). The mutation frequencies vary greatly among SWI/SNF subunits and cancer types, emphasizing the importance of cellular context and SWI/SNF complex composition. Selective pressure in cancer can be expected to particularly benefit mutations that prevent early lineage transitions and maintain an immortal stem or progenitor state. At the same time, mutations that sustain cell proliferation are near universally present in human cancer (Hanahan and Weinberg, 2011). Further studies will be needed to understand the cell-type-specific and combinatorial activities of SWI/SNF components and transcription factors in proliferation versus differentiation decisions, and their interplay with cell-cycle control genes in human cancer.

EXPERIMENTAL PROCEDURES

Strains and Culture

The genotypes of all strains used in this study are listed in Table S7.

RNA-Mediated Interference and Molecular Cloning

Detailed descriptions of the RNAi procedures and all vector and transgene constructions are included in the Supplemental Experimental Procedures.

Immunohistochemical Analysis

For immunostaining with antibodies, animals were fixed using the Bouin's fixative protocol and stained according to standard protocol. EdU incorporation and detection was used to visualize DNA replication during later stages of development (van den Heuvel and Kipreos, 2012). Subsequently, immunostaining with antibodies was performed to identify GFP-positive cells. See Supplemental Experimental Procedures for detailed descriptions.

Microscopy and Quantification of Cell Numbers

Cell division events were quantified by counting the number of GFP-positive cells in the intestine or mesoblast lineage. For relatively weak phenotypes, mesoblast descendants were counted in the region around the vulva. For stronger phenotypes, we counted the total number of eGFP-positive cells, as indicated in the text and figures. Image acquisition and quantifications of mesoblast descendants expressing the *Pcye-1::tagBFP* or *Phlh-8::tagBFP* transcriptional reporters, UNC-15 paramyosin or actin are described in the Supplemental Experimental Procedures.

Single-Molecule Fluorescence in Situ Hybridization

Probes for RNA single-molecule fluorescence in situ hybridization (smFISH) were ordered from Stellaris (http://singlemoleculefish.com/). For quantification of the number of mRNA molecules, the presence of tetramethylrhodamine (TMR) (eGFP) spots was used to draw a region of interest around M-lineage muscle. The number of Cy5 fluorescent mRNA spots was quantified in this region. Further experimental details are provided in the Supplemental Experimental Procedures.

Statistical Analysis

Sample sizes were not pre-determined; instead, all available animals of the right stage and genotype were counted. smFISH data are included from at least eight independent animals, reporter expression and cell numbers from at least ten independent animals. Graphs and data analysis were produced using GraphPad Prism 5. Plots indicate all data points, as well as the mean (average) ± SEM. As the data essentially fit normal distributions, unpaired two-tailed Student's t tests were used to examine statistical significance of the difference between means.

absent); arrowheads indicate mesoblast descendants (green) expressing actin (red) or paramyosin (red). *Mesoblast descendants (green), without expression of actin (red) or paramyosin (red).

(E and G) Percentage of cells with well-organized myofilaments (light gray), aberrant morphology of myofilaments (middle gray), or absence of myofilaments (dark gray) based on actin (E) or paramyosin (G) staining in animals of the indicated genotypes (bottom).

Graphs show mean ± SEM. Scale bars, 20 μm. See also Figure S7.

SUPPLEMENTAL INFORMATION

Supplemental Information includes Supplemental Experimental Procedures, seven figures, and seven tables and can be found with this article online at http://dx.doi.org/10.1016/j.cell.2015.06.013.

AUTHOR CONTRIBUTIONS

S.R. performed all experiments. S.v.d.H. and S.R. designed the experiments, analyzed the data, and wrote the manuscript.

ACKNOWLEDGMENTS

We thank A. Akhmanova, H. Sawa, S. Mitani, A. Hyman, A. Pozniakovsky, G. Wachsman, and B. Scheres for reagents and strains; T. Middelkoop, M. Bienko, A. van Oudenaarden, and the Hubrecht Imaging Center for assistance with smFISH experiments; C. Riedel for access to SWI/SNF ChIP data; M. Boxem for help with data analysis; F. Holstege, M. Boxem, I. The, and A. Thomas for critically reading the manuscript; and members of the van den Heuvel and Boxem groups for help and discussion. Several strains were provided by the CGC, which is funded by the NIH Office of Research Infrastructure Programs (P40 OD010440). This work is part of research program 819.02.016, financed by the Netherlands Organization for Scientific Research (NWO).

Received: November 21, 2014
Revised: March 10, 2015
Accepted: May 14, 2015
Published: July 2, 2015

REFERENCES

Boxem, M., and van den Heuvel, S. (2001). lin-35 Rb and cki-1 Cip/Kip cooperate in developmental regulation of G1 progression in C. elegans. Development *128*, 4349–4359.

Boxem, M., and van den Heuvel, S. (2002). C. elegans class B synthetic multivulva genes act in G(1) regulation. Curr. Biol. *12*, 906–911.

Boyle, A.P., Araya, C.L., Brdlik, C., Cayting, P., Cheng, C., Cheng, Y., Gardner, K., Hillier, L.W., Janette, J., Jiang, L., et al. (2014). Comparative analysis of regulatory information and circuits across distant species. Nature *512*, 453–456.

Buttitta, L.A., and Edgar, B.A. (2007). Mechanisms controlling cell cycle exit upon terminal differentiation. Curr. Opin. Cell Biol. *19*, 697–704.

Chai, J., Charboneau, A.L., Betz, B.L., and Weissman, B.E. (2005). Loss of the hSNF5 gene concomitantly inactivates p21CIP/WAF1 and p16INK4a activity associated with replicative senescence in A204 rhabdoid tumor cells. Cancer Res. *65*, 10192–10198.

Corsi, A.K., Kostas, S.A., Fire, A., and Krause, M. (2000). Caenorhabditis elegans twist plays an essential role in non-striated muscle development. Development *127*, 2041–2051.

de la Serna, I.L., Carlson, K.A., and Imbalzano, A.N. (2001). Mammalian SWI/SNF complexes promote MyoD-mediated muscle differentiation. Nat. Genet. *27*, 187–190.

Eroglu, E., Burkard, T.R., Jiang, Y., Saini, N., Homem, C.C.F., Reichert, H., and Knoblich, J.A. (2014). SWI/SNF complex prevents lineage reversion and induces temporal patterning in neural stem cells. Cell *156*, 1259–1273.

Fay, D.S., Keenan, S., and Han, M. (2002). fzr-1 and lin-35/Rb function redundantly to control cell proliferation in C. elegans as revealed by a nonbiased synthetic screen. Genes Dev. *16*, 503–517.

Fukuyama, M., Gendreau, S.B., Derry, W.B., and Rothman, J.H. (2003). Essential embryonic roles of the CKI-1 cyclin-dependent kinase inhibitor in cell-cycle exit and morphogenesis in C elegans. Dev. Biol. *260*, 273–286.

Gaydos, L.J., Rechtsteiner, A., Egelhofer, T.A., Carroll, C.R., and Strome, S. (2012). Antagonism between MES-4 and Polycomb repressive complex 2 promotes appropriate gene expression in C. elegans germ cells. Cell Rep. *2*, 1169–1177.

Hanahan, D., and Weinberg, R.A. (2011). Hallmarks of cancer: the next generation. Cell *144*, 646–674.

Hebeisen, M., and Roy, R. (2008). CDC-25.1 stability is regulated by distinct domains to restrict cell division during embryogenesis in C. elegans. Development *135*, 1259–1269.

Hedgecock, E.M., and White, J.G. (1985). Polyploid tissues in the nematode Caenorhabditis elegans. Dev. Biol. *107*, 128–133.

Hong, Y., Roy, R., and Ambros, V. (1998). Developmental regulation of a cyclin-dependent kinase inhibitor controls postembryonic cell cycle progression in Caenorhabditis elegans. Development *125*, 3585–3597.

Kadoch, C., Hargreaves, D.C., Hodges, C., Elias, L., Ho, L., Ranish, J., and Crabtree, G.R. (2013). Proteomic and bioinformatic analysis of mammalian SWI/SNF complexes identifies extensive roles in human malignancy. Nat. Genet. *45*, 592–601.

Kandoth, C., McLellan, M.D., Vandin, F., Ye, K., Niu, B., Lu, C., Xie, M., Zhang, Q., McMichael, J.F., Wyczalkowski, M.A., et al. (2013). Mutational landscape and significance across 12 major cancer types. Nature *502*, 333–339.

Kia, S.K., Gorski, M.M., Giannakopoulos, S., and Verrijzer, C.P. (2008). SWI/SNF mediates polycomb eviction and epigenetic reprogramming of the INK4b-ARF-INK4a locus. Mol. Cell. Biol. *28*, 3457–3464.

Kipreos, E.T., Lander, L.E., Wing, J.P., He, W.W., and Hedgecock, E.M. (1996). cul-1 is required for cell cycle exit in C. elegans and identifies a novel gene family. Cell *85*, 829–839.

Kipreos, E.T., Gohel, S.P., and Hedgecock, E.M. (2000). The C. elegans F-box/WD-repeat protein LIN-23 functions to limit cell division during development. Development *127*, 5071–5082.

Korzelius, J., The, I., Ruijtenberg, S., Prinsen, M.B.W., Portegijs, V., Middelkoop, T.C., Groot Koerkamp, M.J., Holstege, F.C.P., Boxem, M., and van den Heuvel, S. (2011). Caenorhabditis elegans cyclin D/CDK4 and cyclin E/CDK2 induce distinct cell cycle re-entry programs in differentiated muscle cells. PLoS Genet. *7*, e1002362.

Kuwahara, Y., Wei, D., Durand, J., and Weissman, B.E. (2013). SNF5 reexpression in malignant rhabdoid tumors regulates transcription of target genes by recruitment of SWI/SNF complexes and RNAPII to the transcription start site of their promoters. Mol. Cancer Res. *11*, 251–260.

Lei, H., Fukushige, T., Niu, W., Sarov, M., Reinke, V., and Krause, M. (2010). A widespread distribution of genomic CeMyoD binding sites revealed and cross validated by ChIP-Chip and ChIP-Seq techniques. PLoS ONE *5*, e15898.

Mello, C.C., Kramer, J.M., Stinchcomb, D., and Ambros, V. (1991). Efficient gene transfer in C.elegans: extrachromosomal maintenance and integration of transforming sequences. EMBO J. *10*, 3959–3970.

Puri, P.L., and Mercola, M. (2012). BAF60 A, B, and Cs of muscle determination and renewal. Genes Dev. *26*, 2673–2683.

Riedel, C.G., Dowen, R.H., Lourenco, G.F., Kirienko, N.V., Heimbucher, T., West, J.A., Bowman, S.K., Kingston, R.E., Dillin, A., Asara, J.M., and Ruvkun, G. (2013). DAF-16 employs the chromatin remodeller SWI/SNF to promote stress resistance and longevity. Nat. Cell Biol. *15*, 491–501.

Saito, R.M., Perreault, A., Peach, B., Satterlee, J.S., and van den Heuvel, S. (2004). The CDC-14 phosphatase controls developmental cell-cycle arrest in C. elegans. Nat. Cell Biol. *6*, 777–783.

Sawa, H., Kouike, H., and Okano, H. (2000). Components of the SWI/SNF complex are required for asymmetric cell division in C. elegans. Mol. Cell *6*, 617–624.

Schuettengruber, B., Martinez, A.-M., Iovino, N., and Cavalli, G. (2011). Trithorax group proteins: switching genes on and keeping them active. Nat. Rev. Mol. Cell Biol. *12*, 799–814.

Shibata, Y., Uchida, M., Takeshita, H., Nishiwaki, K., and Sawa, H. (2012). Multiple functions of PBRM-1/Polybromo- and LET-526/Osa-containing chromatin remodeling complexes in C. elegans development. Dev. Biol. *361*, 349–357.

Sulston, J.E., and Horvitz, H.R. (1977). Post-embryonic cell lineages of the nematode, Caenorhabditis elegans. Dev. Biol. *56*, 110–156.

Sulston, J.E., Schierenberg, E., White, J.G., and Thomson, J.N. (1983). The embryonic cell lineage of the nematode Caenorhabditis elegans. Dev. Biol. *100*, 64–119.

The, I., Ruijtenberg, S., Bouchet, B.P., Cristobal, A., Prinsen, M.B.W., van Mourik, T., Koreth, J., Xu, H., Heck, A.J.R., Akhmanova, A., et al. (2015). Rb and FZR1/Cdh1 determine CDK4/6-cyclin D requirement in C. elegans and human cancer cells. Nat. Commun. *6*, 5906.

van den Heuvel, S., and Dyson, N.J. (2008). Conserved functions of the pRB and E2F families. Nat. Rev. Mol. Cell Biol. *9*, 713–724.

van den Heuvel, S., and Kipreos, E.T. (2012). C. elegans cell cycle analysis. Methods Cell Biol. *107*, 265–294.

Wang, D., Kennedy, S., Conte, D., Jr., Kim, J.K., Gabel, H.W., Kamath, R.S., Mello, C.C., and Ruvkun, G. (2005). Somatic misexpression of germline P granules and enhanced RNA interference in retinoblastoma pathway mutants. Nature *436*, 593–597.

Wang, X., Haswell, J.R., and Roberts, C.W.M. (2014). Molecular pathways: SWI/SNF (BAF) complexes are frequently mutated in cancer—mechanisms and potential therapeutic insights. Clin. Cancer Res. *20*, 21–27.

Wilson, B.G., and Roberts, C.W.M. (2011). SWI/SNF nucleosome remodellers and cancer. Nat. Rev. Cancer *11*, 481–492.